Vertical aerosol distribution over Europe: Statistical analysis of Raman lidar data from 10 European Aerosol Research Lidar Network (EARLINET) stations

V. Matthias,[1,2] D. Balis,[3] J. Bösenberg,[1] R. Eixmann,[4] M. Iarlori,[5] L. Komguem,[6] I. Mattis,[7] A. Papayannis,[8] G. Pappalardo,[9] M. R. Perrone,[10] and X. Wang[11]

Received 13 February 2004; revised 12 May 2004; accepted 29 June 2004; published 17 September 2004.

[1] Since 2000, regular lidar observations of the vertical aerosol distribution over Europe have been performed within the framework of EARLINET, the European Aerosol Research Lidar Network. A statistical analysis concerning the vertical distribution of the volume light extinction coefficients of particles derived from Raman lidar measurements at 10 EARLINET stations is presented here. The profiles were measured on a fixed schedule with up to two measurements per week; they typically covered the height range from 500 m to 6000 m above ground level (agl). The analysis is made for the planetary boundary layer (PBL) as well as for several fixed layers above ground. The results show typical values of the aerosol extinction coefficient and the aerosol optical depth (AOD) in different parts of Europe, with highest values in southeastern Europe and lowest values in the northwestern part. Annual cycles and cumulative frequency distributions are also presented. We found that higher aerosol optical depths in southern Europe compared to the northern part are mainly attributed to larger amounts of aerosol in higher altitudes. At 9 of the 10 sites the frequency distribution of the aerosol optical depth in the planetary boundary layer follows a lognormal distribution at the 95% significance level. *INDEX TERMS:* 0305 Atmospheric Composition and Structure: Aerosols and particles (0345, 4801); 0345 Atmospheric Composition and Structure: Pollution—urban and regional (0305); 3309 Meteorology and Atmospheric Dynamics: Climatology (1620); 3360 Meteorology and Atmospheric Dynamics: Remote sensing; *KEYWORDS:* aerosol, Raman lidar, statistical analysis

Citation: Matthias, V., et al. (2004), Vertical aerosol distribution over Europe: Statistical analysis of Raman lidar data from 10 European Aerosol Research Lidar Network (EARLINET) stations, *J. Geophys. Res.*, *109*, D18201, doi:10.1029/2004JD004638.

1. Introduction

[2] Aerosols are known to play a major role in the Earth's climate [*Intergovernmental Panel on Climate Change* (*IPCC*), 2001]. Their influence on the radiation budget is manifold. It covers the direct absorption and scattering of solar and terrestrial radiation [*Charlson et al.*, 1992], as well as indirect effects on cloud microphysical properties, cloud lifetime and precipitation rates [*Twomey*, 1977; *Schwartz and Slingo*, 1996; *Lohmann and Feichter*, 1997]. Additionally, chemical processes in the troposphere are significantly influenced by heterogeneous reactions on the surface of aerosol particles [*Andreae and Crutzen*, 1997].

[3] Despite their indubitable importance in atmospheric physics, significant gaps in the scientific knowledge about aerosols still exist. This is especially true for the vertical distribution of aerosols in the atmosphere, which is of essential relevance to understand aerosol effects on climate [*Kaufman et al.*, 1997]. Data on the vertical aerosol distribution were taken during large field experiments like TARFOX, LACE'98, ACE-1, and ACE-2 [*Russell et al.*, 1999; *Ansmann et al.*, 2002; *Bates et al.*, 1998; *Raes et al.*, 2000], but no attempt was made to derive longer time series of the aerosol vertical distribution on a continental scale until EARLINET (European Aerosol Research Lidar Network) [*Bösenberg et al.*, 2003] was established in 2000. Within the Asian lidar network [*Murayama et al.*, 2001] numerous vertical profiles of the aerosol distribution were retrieved but the network was dedicated to special events (the Asian dust outbreaks) and not to regular observations. The German lidar network [*Bösenberg et al.*, 2001] was established in 1997; it was the first lidar network dedicated to regular observations but it comprised only 5 lidar stations in Germany, covering a scale of a few hundred kilometers. This was not enough to investigate

[1]Max-Planck-Institut für Meteorologie, Hamburg, Germany.
[2]Now at Institute for Coastal Research, GKSS Research Center, Geesthacht, Germany.
[3]Laboratory of Atmospheric Physics, Aristotele University of Thessaloniki, Greece.
[4]Institut für Atmosphärenphysik, Kühlungsborn, Germany.
[5]Dipartimento di Fisica, Universitá Degli Studi, L'Aquila, Italy.
[6]Physics Department, University of Wales, Aberystwyth, UK.
[7]Institut für Troposphärenforschung, Leipzig, Germany.
[8]Lasers and Applications Group, National Technical University of Athens, Greece.
[9]Istituto di Metodologie per l'Analisi Ambientale, CNR, Potenza, Italy.
[10]Dipartimento di Fisica, Universitá di Lecce, Lecce, Italy.
[11]Istituto Nazionale per la Fisica della Materia, Napoli, Italy.

0148-0227/04/2004JD004638

aerosol transport and modification in detail and to observe significant differences between the aerosol distributions at different sites. Some of the methods used in EARLINET, e.g., on quality assurance or data sampling, were developed in this project.

[4] Within EARLINET, coordinated aerosol lidar measurements have been performed at 22 lidar stations in 12 European countries. Most of the profiles are aerosol backscatter coefficient profiles at typically three laser wavelengths in the UV (355 or 351 nm), the visible (532 nm), and the infrared (1064 nm). However, the retrieval of aerosol backscatter coefficients from pure elastic lidar returns suffers from considerable uncertainties due to the unknown extinction-to-backscatter ratio (lidar ratio), which has to be prescribed for the data evaluation. Therefore, in EARLINET, UV Raman lidar measurements of the aerosol extinction coefficient [*Ansmann et al.*, 1992] are the preferred method to derive aerosol optical properties in a quantitative way. This method allows also the determination of aerosol extinction coefficients below clouds, because a calibration of the lidar profiles in an aerosol free region is not necessary. Additionally, an aerosol backscatter profile can be determined down to very low altitudes above ground using the quotient of elastic and Raman backscatter of one emission wavelength. So Raman lidar measurements provide also lidar ratio profiles and give the possibility to classify the aerosol type. At 10 EARLINET stations regular Raman lidar measurements at 355/351 nm were conducted between May 2000 and December 2002. Because of the low atmospheric Raman backscatter, the measurements were taken around sunset at low solar background conditions. Nevertheless, they are still representative for the fully developed boundary layer in the afternoon.

[5] Besides the mentioned homogeneous sampling, the statistical analysis of aerosol lidar data from 10 different stations requires an extensive quality assurance procedure including direct comparisons of the participating lidar systems. This is of special importance because the lidar systems used in EARLINET differ in several technical aspects like telescope size, detectors and amplifiers and the optical arrangement. In EARLINET, lidar systems were quality assured by performing direct intercomparisons of at least two systems at a time at one place [*Matthias et al.*, 2004]. Aerosol backscatter [*Böckmann et al.*, 2004] and aerosol extinction algorithms [*Pappalardo et al.*, 2004] were compared separately using synthetic lidar data. The results showed that typical error margins are in the order of 10–15%, depending on height and signal statistics. Systematic errors were mainly observed in the lowest altitudes where an incomplete overlap between the emitted laser beam and the telescope field of view can lead to an underestimation of aerosol backscatter and extinction coefficients. The aerosol extinction profiles stored in the database start at about 500 m above ground or higher.

[6] This paper describes the statistical analysis of aerosol extinction coefficient profiles from 10 EARLINET stations which provided data from at least 19 months between May 2000 and December 2002. These data allow also quantitative statements about the vertical aerosol distribution over Europe.

[7] An overview of the used data is presented in section 2 and the evaluation methods are described in section 3.

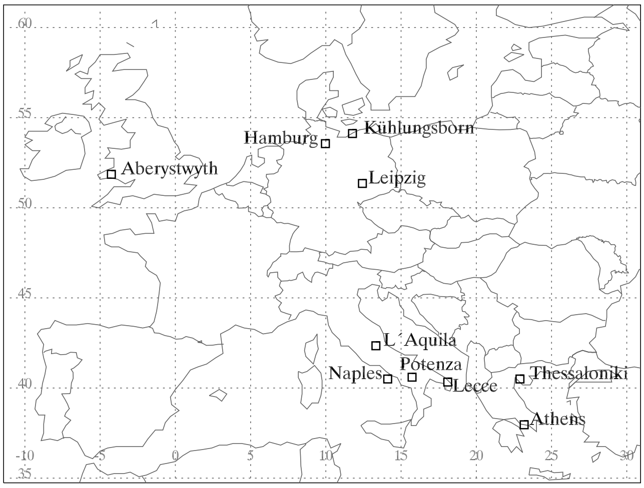

Figure 1. Geographical location of the 10 EARLINET stations considered in this study.

Section 4 describes the main results and interpretations. A summary is given in section 5.

2. Database

[8] The statistical analysis of the vertical profiles of the aerosol extinction coefficient derived in EARLINET is restricted to the regular measurements. These measurements have been taken at each lidar station two times a week on preselected days (Mondays and Thursdays) and time windows (one hour before and up to three hours after sunset). Additional measurements performed on other days, e.g., for the observation of diurnal cycles or special events are not included in the statistical analysis to avoid a bias for those "special" situations and for fair weather periods. Only one profile, typically a 30 min. average, is considered in each of the predefined measurement windows.

[9] Low and midrange clouds are excluded in all lidar profiles stored in the EARLINET database. Cirrus layers included in the aerosol profiles can easily be identified by the strong backscatter and the more inhomogeneous structure compared to aerosol layers. Cirrus clouds are not considered for this study and a possible enhancement of the aerosol extinction coefficient at higher altitudes due to the presence of such clouds can be excluded.

[10] All data were taken between 1 May 2000 and 31 December 2002. Because of technical reasons and meteorological conditions at the individual sites the data sets can be quite different in number of profiles, vertical extent and seasonal coverage. Raman channels for example were included in some systems in the second half of 2000 and therefore measurements cover only the period from October/November 2000 to November/December 2002. The geographical location of the stations in Europe is shown in Figure 1. The number of measurements performed at each station are presented in Table 1. Numbers are also given for the summer (April until September) and winter (October until March) periods to show the seasonal variation of the number of considered profiles. Eight stations cover at least a period of 2 years. In Thessaloniki measurements started only in February 2001. Aerosol extinction

Table 1. Number of Measurements, Covered Time Periods, and Number of Considered Measurements in Three Altitude Intervals for 10 EARLINET Raman Lidar Stations

Station	Abbreviation	Covered Time	All	Summer	Winter	0–1 km	1–2 km	2–5 km
Aberystwyth	ab	May 2000 to Nov. 2002	55	34	21	53	55	27
Athens	at	Nov. 2000 to Nov. 2002	81	45	36	79	61	9
Hamburg	hh	May 2000 to Nov. 2002	109	71	38	103	84	48
Kühlungsborn	kb	May 2000 to Nov. 2002	62	39	23	0	45	50
L'Aquila	la	May 2001 to Nov. 2002	75	41	34	75	75	7
Lecce	lc	May 2000 to Aug. 2002	166	94	72	162	137	24
Leipzig	le	May 2000 to Dec. 2002	83	55	28	8	77	81
Naples	na	Oct. 2000 to Dec. 2002	145	64	81	141	143	69
Potenza	po	May 2000 to Dec. 2002	88	60	28	26	85	75
Thessaloniki	th	Feb. 2001 to Nov. 2002	58	31	27	50	55	30

coefficients from L'Aquila were available since May 2001, before that date the full overlap of the system was above 3000 m. Usually most of the profiles were taken in the summer period, which is partly because three summers and only two winters fall in the measurement period of 7 stations. However, especially in northern Europe weather conditions also play a major role in the seasonal distribution of the measurements.

3. Statistical Methods

[11] The statistical evaluation follows the methods described by *Matthias and Bösenberg* [2002]. It is done for the planetary boundary layer (PBL) where most of the aerosol particles can be found and for a fixed layer of 2 km above ground. Seven out of 10 stations deliver profiles from ~500 m agl upward. The other three stations can deliver only a limited number or even no extinction values in the lowest 1000 m above ground (Table 1). The aerosol optical depth (AOD) in the PBL and the 2 km layer is derived by extrapolating the lowest data point down to ground assuming constant values of the aerosol extinction coefficient in this lowest layer. Then, the values are integrated over the whole layer. In most cases, this assumption can be made without large errors because the boundary layer is usually still well mixed at sunset when the measurements are taken. However, in some winter cases the lowest measurement height is above the boundary layer and representative extinction coefficients can not be determined for the lowest layer. Fortunately, those cases are rare and, thus they are excluded from our statistical analysis. The 2–5 km region is not always covered by the measurements. The main reason for this are low and midrange clouds that limit the evaluation range of the lidar data and the low signal statistics in upper altitudes for most of the systems. Above 5 km, the number of measurements that can be used for the statistics is too low at most of the stations. The presence of aerosol layers in those altitudes is not very frequent, but long-range transport of, e.g., Saharan dust, biomass burning aerosol or boundary layer aerosol from North America are occasionally observed above 5 km. A statistics of these cases is not within the scope of this paper.

[12] The error in the optical depth values is mainly determined by the statistical error of the aerosol extinction coefficient profile. It is typically on the order of 10–15% and depends on temporal and spatial averaging. In cases when the PBL is not well mixed or is not covered by the lidar measurement, additional errors in the optical depth determination are introduced by the extrapolation of the lowest extinction coefficient down to ground. Obviously, these errors vary from case to case and can be up to 100% (if the PBL is not covered at all). Typical errors are estimated to be ~10% or 0.03 in the optical depth, whichever is larger, giving an overall error of the AOD values of ~20% or 0.05 in the optical depth [*Matthias et al.*, 2004].

[13] The PBL height itself is also subject of the statistical analysis. In this paper we use PBL height for that height below which most of the aerosol is confined, even if this layer is not in every case a well mixed layer. Additional layers in higher altitudes, mostly containing aerosol from long-range transport, are treated separately. Although the extinction measurements were performed after sunset, they still represent the afternoon conditions with a fully developed boundary layer very well. This was regularly verified by comparisons with pure backscatter measurements taken 2–3 hours after noon.

[14] The determination of the boundary layer height out of the lidar data is done by looking at the first significant negative gradient in the range-corrected lidar signal, starting from ground. An example is given in Figure 2 for a measurement taken on 12 September 2002, 1848–1913 UT, at Hamburg. The range-corrected signal at 355 nm (PR^2, P being the lidar signal and R the range) is given together with the gradient of the signal ($\frac{d}{dR}PR^2$). The signal is averaged 240 m in altitude, which is a typical

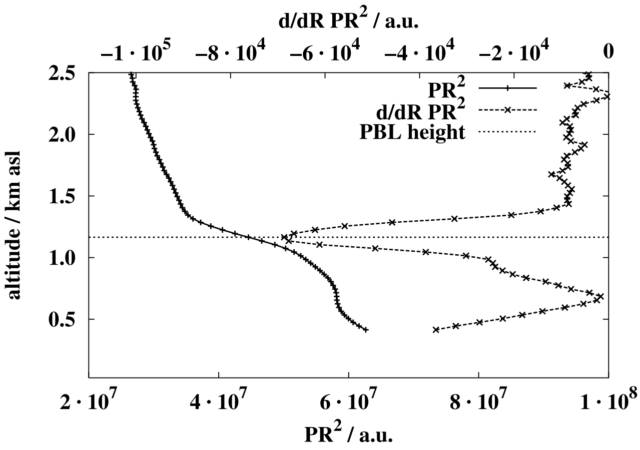

Figure 2. Range-corrected lidar signal PR^2 and its gradient $\frac{d}{dR}PR^2$ at 355 nm. The measurement was taken on 12 September 2002, 1848–1913 UT, at Hamburg. Vertical averaging is 240 m, and the data resolution is 30 m. The PBL height was determined to 1165 m asl.

Table 2. Statistical Parameters of the Planetary Boundary Layer (PBL) Height for 10 EARLINET Stations

Station	PBL Height, m agl	SD, m	Relative SD	Skewness
Aberystwyth	1204	481	0.40	0.62
Hamburg	1242	506	0.41	0.62
Kühlungsborn	1984	566	0.29	0.36
Leipzig	1937	796	0.41	−0.07
L'Aquila	1742	509	0.29	0.18
Lecce	1261	599	0.48	1.29
Naples	1442	626	0.43	0.70
Potenza	1542	304	0.20	0.69
Athens	1172	319	0.27	1.16
Thessaloniki	1363	416	0.31	0.74

averaging length for Raman lidar measurements. The used data resolution is 30 m. The steep gradient in the range corrected lidar signal results from the high decrease in aerosol backscatter caused by lower particle concentration and humidity above the PBL. In this case a PBL height of 1165 m asl was determined. The method is very simple and it has been used in one or the other form since many years [*Russell et al.*, 1974; *Flamant et al.*, 1997; *Menut et al.*, 1999]. It was validated against other methods to derive the PBL height [*Coulter*, 1979; *Kaimal et al.*, 1982] showing good agreement under well mixed conditions. It can also be used down to altitudes where no extinction determination is possible, if a correction of the incomplete overlap is applied to the measured signal [*Wandinger and Ansmann*, 2002].

[15] In the case of Raman lidars the aerosol backscatter coefficient can also be used to determine the PBL height. The backscatter coefficient profile is calculated from a signal ratio profile [*Ansmann et al.*, 1992] so that overlap effects widely cancel out. Therefore, even in situations with rather low PBL height, well below the minimum measurement height, the top height of the PBL is identified based on the backscatter profile.

[16] Nevertheless, the method can fail at locations where special circulation patterns like sea breeze effects or orographic effects play a major role or in the evening when a stabilization due to radiative cooling can be observed in the lowest few hundred meters. Therefore, if the PBL height could not be clearly identified with the gradient method, the time series of the lidar signals, also from afternoon measurements, could be used to get additional information about the existence of mixing processes.

[17] However, the necessary automated detection of the PBL height by an algorithm is not easy to implement and can be associated with considerable errors, e.g., if the signal intensity is low and large statistical fluctuations cause sharp gradients in the profile. The algorithm used requires the definition of threshold values and the results also depend on data averaging and spatial resolution of the range-corrected signals. Therefore in addition to the PBL also the layer up to 2 km above the lidar site is statistically evaluated in the same way. A comparison between these approaches gives higher confidence in the results for one of the layers. Additionally it simplifies the comparison of lidar data with results from global climate models, which typically do not resolve the planetary boundary layer.

[18] The aerosol optical depth is calculated for fixed layers of 0–1 km, 1–2 km, 2–5 km above ground level and the vertical distribution of the aerosol exinction is derived from this. Higher layers are not considered here because they are often not covered by the Raman lidar measurements and the statistics would be based on only few measurements. Additionally, elastic lidar measurements show that the contribution of aerosol particles in those very high layers to the total AOD is rather small.

[19] For the lowest layer of the vertical distribution (0–1 km), the optical depth values are calculated by assuming the aerosol extinction coefficient closest to ground to represent the extinction in the missing heights. If no extinction value was measured in the lowest layer, the profile is not considered for that range. For the other layers, only profiles which cover the whole height range are taken; see Table 1 for the fraction of all measurements in the individual intervals. So the values in the different ranges represent the mean of the available profiles in that height range.

4. Results

[20] Aerosol extinction coefficient measurements from the 10 aforementioned EARLINET stations are the basis for investigations about the PBL height and the aerosol optical depth in the PBL, the 2 km layer and three fixed height layers. Statistical parameters like mean, median, standard deviation and skewness are derived for the PBL and the 2 km layer. Distribution functions and mean annual cycles are also shown. A 10 weeks (70 days) running average is applied to the data to better recognize the main features. This averaging length ensures that no gaps remain in the averaged data set.

4.1. PBL Height

[21] The PBL height shows in most cases a clear annual cycle with higher values in summer than in winter. For example, for Hamburg it has been shown from previous measurements that on average this cycle follows quite well a sine function with maximum values in the beginning of July and lowest values around beginning of January [*Matthias and Bösenberg*, 2002]. The variability of the PBL height is high, usually with a relative standard deviation on the order of 0.4 (Table 2). However, there are also stations where the annual cycle of the PBL height shows only a weak dependence on season, like Athens, or even lower values in summer than in winter, like Lecce (Figures 3a–3j). The reasons for the surprising feature in Lecce is not yet clear. A possible reason which is under investigation for the low summer values are sea breeze effects leading to an additional layer representing the mixing height over the sea. Very low PBL heights in winter might not be detected and instead weak gradients in the aerosol distribution in upper layers are interpreted as the PBL height. The results from Kühlungsborn are clearly influenced by the difficulty associated with covering the lowest 1500 m of the troposphere, which leads to an overestimation of the mean PBL height and a rather low variability. Leipzig is the only station which is not close to the coast or in the mountains. It shows highest PBL heights which are clearly influenced by the more pronounced convection over the continent. High mean PBL heights and low variability can also be found for Potenza and L'Aquila, both mountain stations at 820 m and 683 m above sea level (asl), respectively. All measurements showed that the top of the PBL is rarely above 3000 m asl, therefore mountain

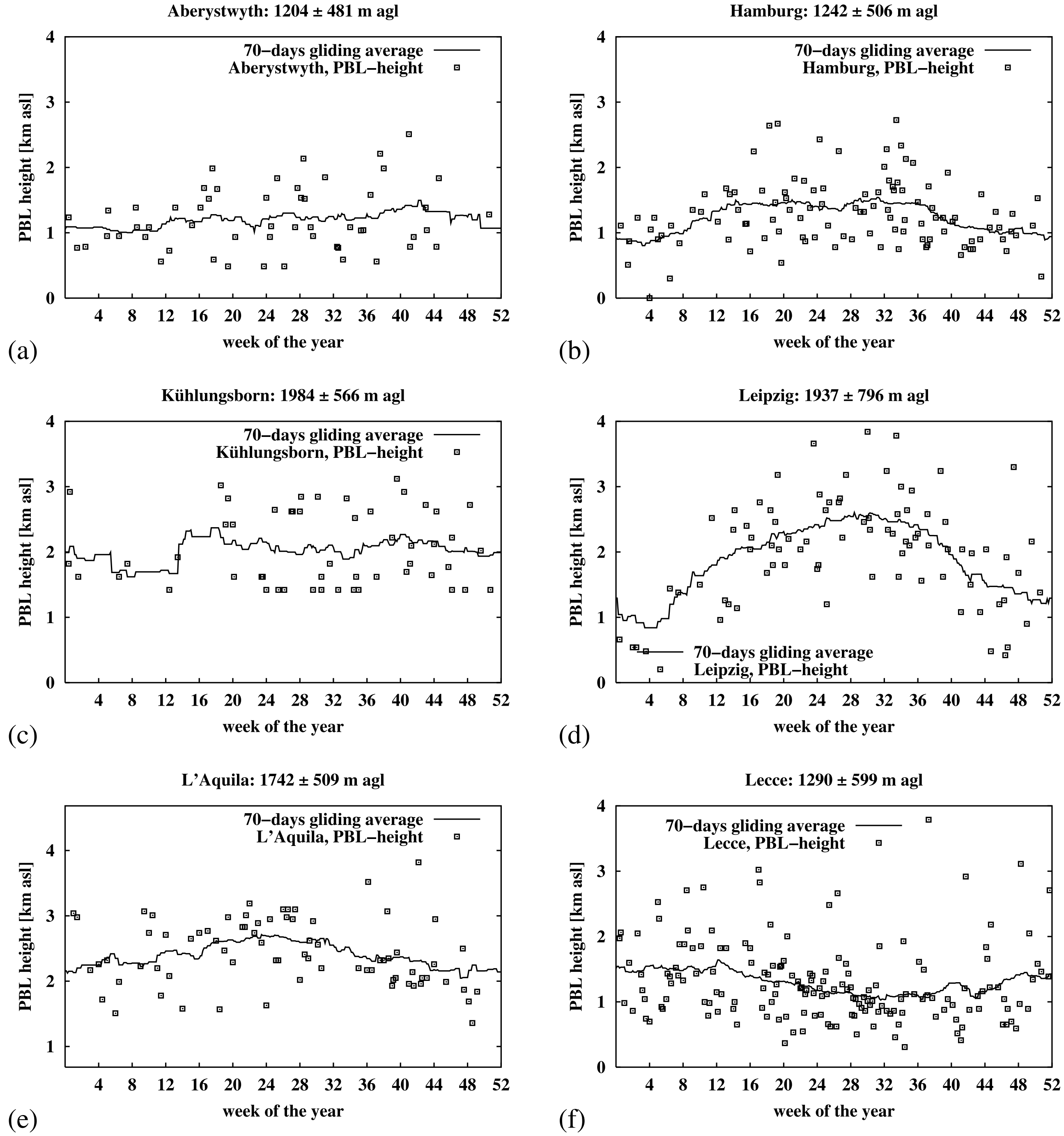

Figure 3. Annual cycle of the planetary boundary layer height for 10 EARLINET stations. For the mountain stations, L'Aquila and Potenza, the PBL height scale has been adjusted to ground level.

stations have a cutoff for high PBL heights compared to low-level stations. Low mean values and also low variability are found for Athens, which can be explained by the strong influence of local circulation patterns due to the surrounding mountains.

4.2. Aerosol Optical Depth

[22] For all 10 stations considered the aerosol optical depth at 355/351 nm is calculated in the planetary boundary layer, the 2 km layer and in fixed layers of 0–1 km, 1–2 km and 2–5 km above ground level. AOD values in the PBL range from 0.16 (Aberystwyth) to 0.45 (Thessaloniki) with high variability throughout the whole year (see Table 3 and Figures 4a–4j). The relative standard deviation is typically between 0.5 for southern European sites and 0.8 for northern European ones. Again, Kühlungsborn is an exception with lowest values and highest variability which can also be explained by missing values for PBL heights below 1500 m. Thessaloniki shows exceptionally high values and highest fluctuations in southern Europe. Additionally it is the only station where an AOD >1 was occasionally observed. In summer 2001, biomass burning aerosols orig-

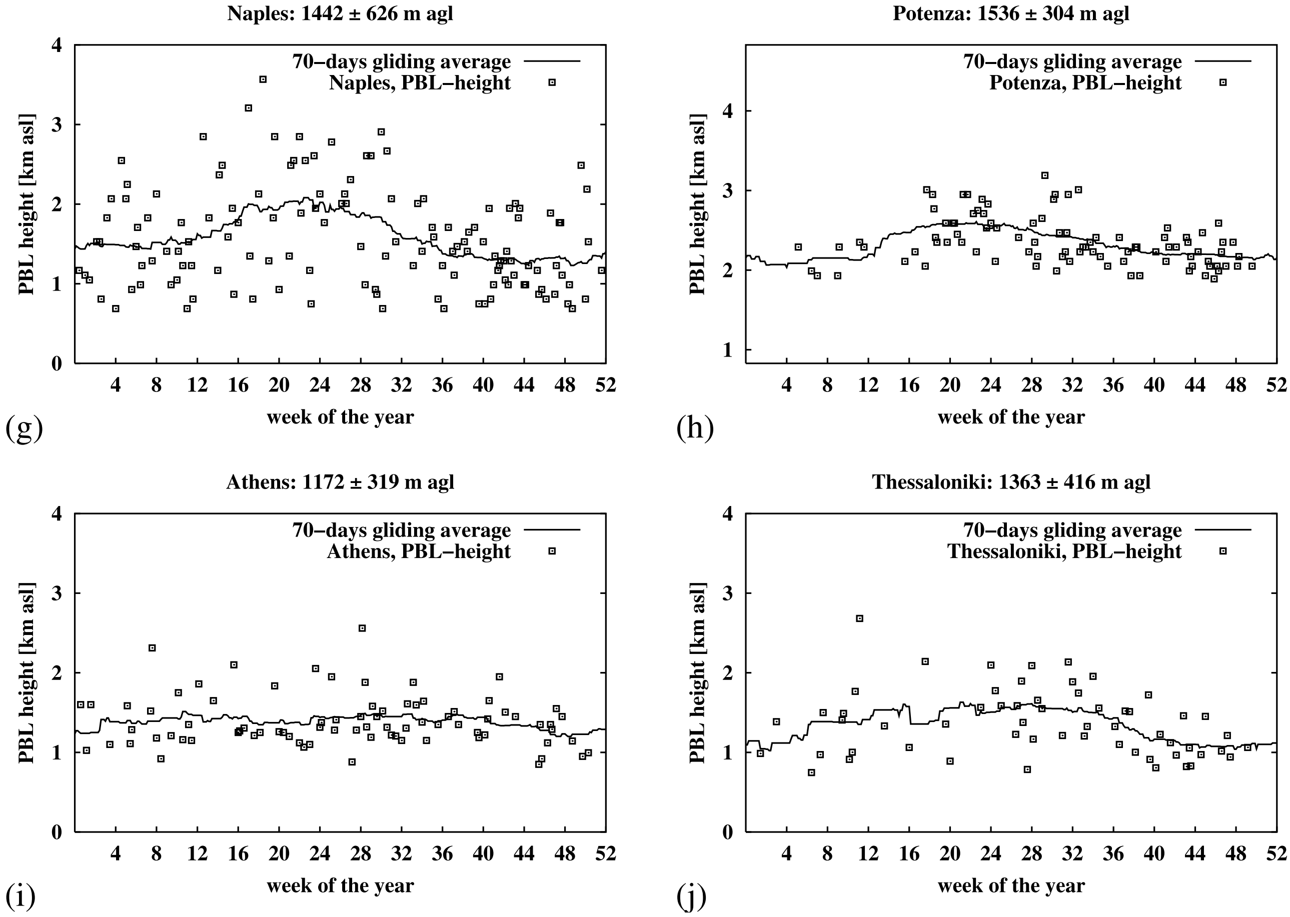

Figure 3. (continued)

inating from the Black Sea region were observed over Thessaloniki [*Balis et al.*, 2003]. These events contributed considerably to high AOD values at that time.

[23] Generally, higher values of the aerosol optical depth can be found in summer compared to winter, which is at least partly due to higher PBL heights in summer. Hamburg, Kühlungsborn and Leipzig show an interesting annual cycle of the AOD with two maxima, one in spring and one in late summer/early fall. It can only be speculated whether, e.g., typical flow patterns in Germany, agricultural activities or humidity effects are responsible for this feature.

[24] All distribution functions show positive skewness (see Table 3). Again higher values are found for the northern stations (0.9–1.9) and lower values for the southern European ones (0.5–1.0). Kühlungsborn differs for known reasons from the general pattern with exceptionally high values for both standard deviation and skewness. Also the frequency distribution from Thessaloniki shows a remarkably high skewness, which is caused by the occasionally observed very high AOD values.

[25] The high skewness at all stations already indicates that the frequency distribution is not Gaussian. In fact, it has been shown that the lognormal distribution represents the cumulative frequency distribution of the AOD much better than a Gaussian distribution does (Figures 5a–5j). Two tests are applied to check the quality of the fitted distribution function, the χ^2 test and the Kolmogorov-Smirnov test. The χ^2 test looks for quadratic deviations of the measurements from the fitted distribution in predefined classes (here optical depth intervals) while the Kolmogorov-Smirnov test looks for maximum deviations in the same classes. For both tests, threshold values for a significance level of 95% are given in tables [*Johnson and Leone*, 1964]. Following these tests, the Kolmogorov-Smirnov test is passed by all stations. For the χ^2 test the result depends on the number of classes (optical depth intervals) defined for the test calculations. Since it is recommended to have at least five elements in each class, in the beginning nine classes were defined and 7 of the 10 groups passed the test. After reducing the number of classes to seven, two additional groups passed the test. Only the frequency distribution of Lecce cannot be

Table 3. Statistical Parameters of the Aerosol Optical Depth (AOD) in the PBL and the 2 km Layer for 10 EARLINET Stations

	Mean AOD		SD		Relative SD		Skewness	
Station	PBL	2 km	PBL	2 km	PBL	2 km	PBL	2 km
Aberystwyth	0.16	0.23	0.13	0.16	0.81	0.70	1.86	1.29
Hamburg	0.26	0.29	0.22	0.20	0.83	0.69	1.90	1.90
Kühlungsborn	0.14	0.14	0.19	0.17	1.38	1.21	2.82	1.89
Leipzig	0.30	0.28	0.23	0.19	0.89	0.68	0.94	0.97
L'Aquila	0.32	0.35	0.14	0.15	0.44	0.44	0.49	0.74
Lecce	0.25	0.32	0.13	0.14	0.54	0.44	0.92	0.65
Naples	0.24	0.27	0.15	0.15	0.62	0.56	1.02	0.77
Potenza	0.22	0.27	0.10	0.11	0.44	0.41	0.48	0.27
Athens	0.30	0.43	0.13	0.18	0.44	0.42	0.94	0.67
Thessaloniki	0.45	0.58	0.39	0.43	0.87	0.73	2.68	2.15

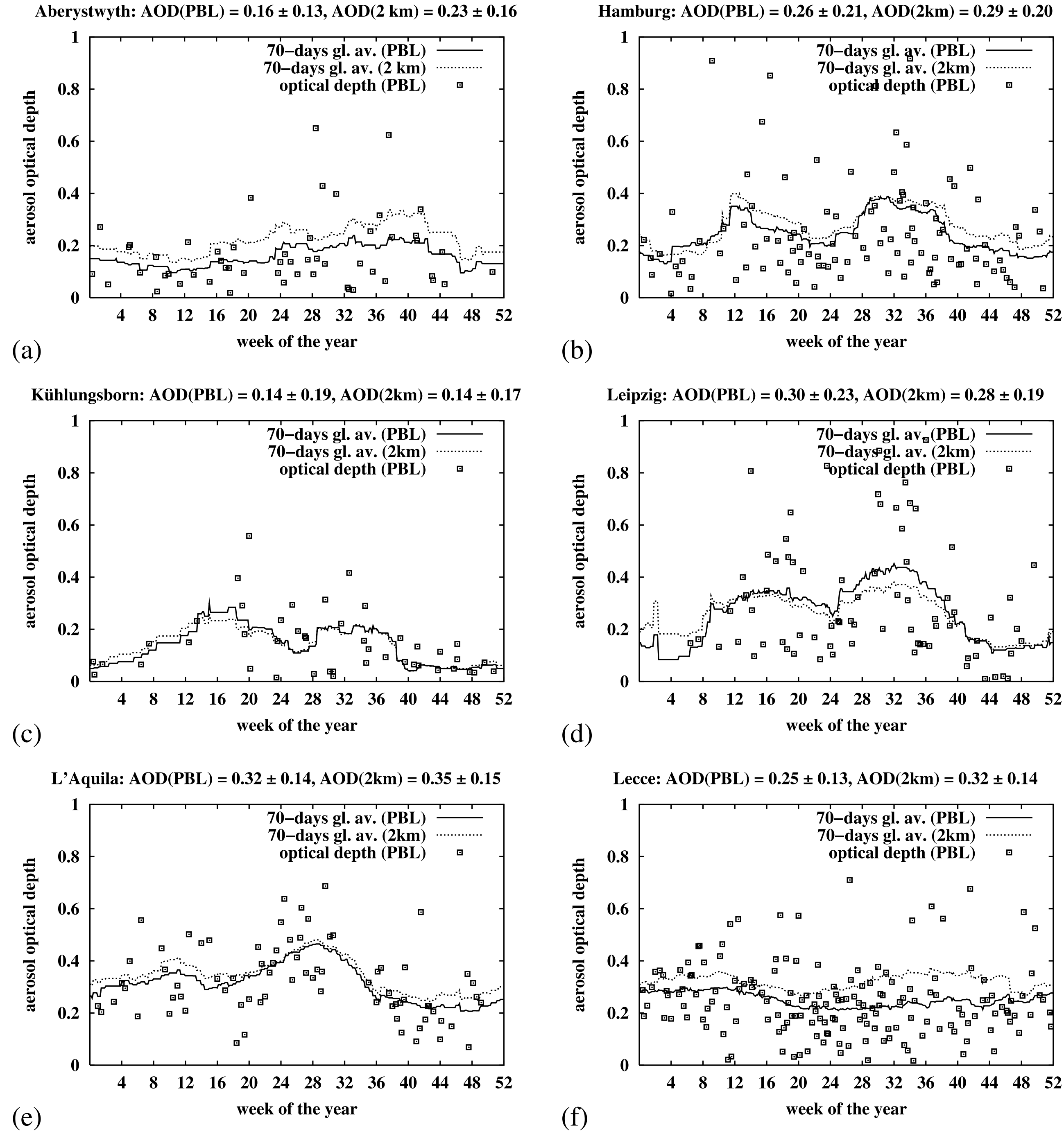

Figure 4. Annual cycle of the aerosol optical depth at 355/351 nm in the planetary boundary layer and in the layer 2 km above ground for 10 EARLINET stations.

represented by a lognormal distribution on the 95% significance level. This is possibly related to the special circulation patterns at this place. Lognormal distributions for the aerosol optical depth have also been found at other places, using AERONET Sun photometer data [*O'Neill et al.*, 2000]. In Table 4 the median values and the 69% (1σ) intervals of the distribution functions are given. Calculated medians fit the measurements quite well, the 1σ intervals are usually very broad and cover values from approximately 0.08 to 0.45. In Thessaloniki and Leipzig, higher values of 0.5 and more can be found in the 1σ interval.

[26] The analysis of the 2 km layer and the comparison to the PBL can be seen in Table 3 and Figures 4a–4j. At 8 of the 10 stations the optical depth in the 2 km layer is slightly enhanced compared to the PBL because small amounts of free tropospheric aerosol are included if the PBL top is below 2 km. Because lower PBL heights are found in winter, the AOD is typically more enhanced in winter than in summer (e.g., Hamburg, L'Aquila, Naples, Figures 4b, 4e, and 4g). No difference at all can be seen at Kühlungsborn which is consistent with the overestimated PBL heights. At Leipzig, summer values are slightly decreased

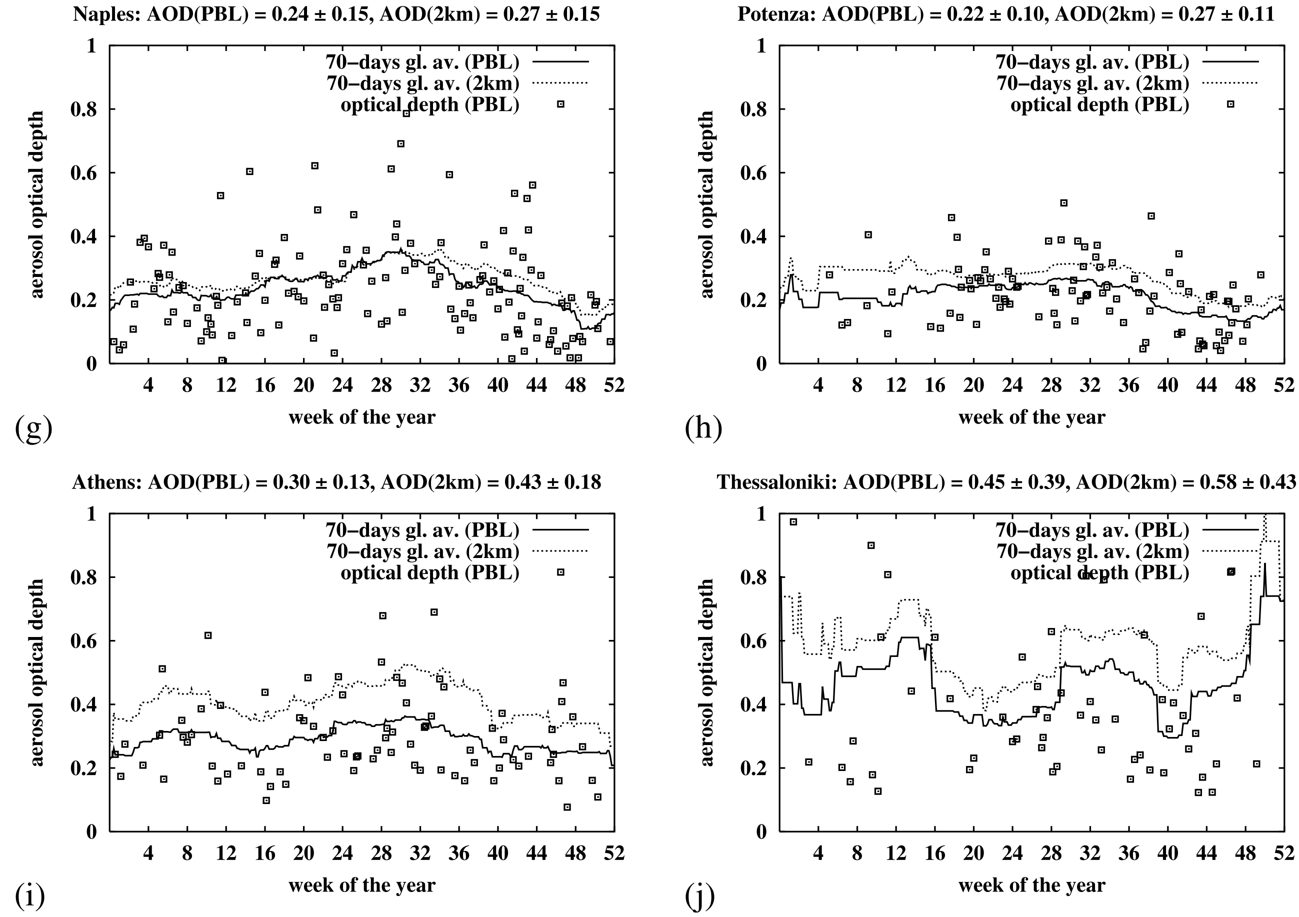

Figure 4. (continued)

which is due to the high PBL heights that are found in summer. The largest enhancement of the AOD values is found at Athens and Thessaloniki. Here, a large part of the aerosol is not confined in the layer that is believed to be the PBL. Partly, this will be due to the low PBL heights estimated from the elastic lidar signals. Possibly the typical aerosol layering at those sites does not allow a reliable detection of the correct PBL height. Another important effect is the presence of Saharan dust in comparably low altitudes. Saharan dust is frequently found over Greece and due to the relatively short transport path, it can also be detected at comparatively low altitudes below 2 km [*Papayannis et al.*, 2001; *Kalabokas et al.*, 2002]. However, Italy is also considerably influenced by Saharan dust events [*De Tomasi et al.*, 2003] but none of the stations shows these large differences between the AOD in the PBL and in the 2 km layer. These results show the difficulty of comparing the AOD values in the PBL among the different stations and support the additional investigation of the 2 km layer. The determination of the PBL height at the different stations can be treated in different ways by the data producers and is in some cases subject to an individual judgment. Better comparibility of the AOD values among the stations is given by the fixed layers.

[27] The relative standard deviation is lower for the 2 km layer than for the PBL. This follows from the enhancement of the low values in winter and a possible decrease of some summer values where high PBL tops were detected. The skewness does not show a common picture. It is reduced in the 2 km layer at most of the stations but the distributions still follow the lognormal approach (see Figures 5a–5j). Here the Kolmogorov-Smirnov test was again passed by all stations while the χ^2 test for nine classes was only passed by 7 of the 10 stations. After a further reduction of the classes to six also these three stations passed the test on the 95% significance level.

[28] The differences in the 1σ intervals for the AOD in the PBL and in the 2 km layer are not very large. Although median values are in 8 of the 10 cases shifted to larger values, only three stations (Aberystwyth, Athens and Thessaloniki) show a significantly larger 1σ interval (more than 0.02 enhanced, Table 4). The large spread of the values demonstrates the large variability of possible aerosol optical depth values, even in the planetary boundary layer where some aerosol is always present. The typical duration of a few weeks for field experiments is not enough to get a representative sample of the aerosol distribution over Europe. Only long-term measurements on a regular basis can give information about the real variability and about trends.

[29] Additional to the column values, the vertical distribution of the aerosol extinction coefficient is investigated for the three layers 0–1 km, 1–2 km, and 2–5 km (Figure 6). The mean values shown here represent different numbers of profiles. Three stations provided few or even no measurements in the 0–1 km range; in the range 1–2 km the coverage is very good for all stations; and the layer 2–

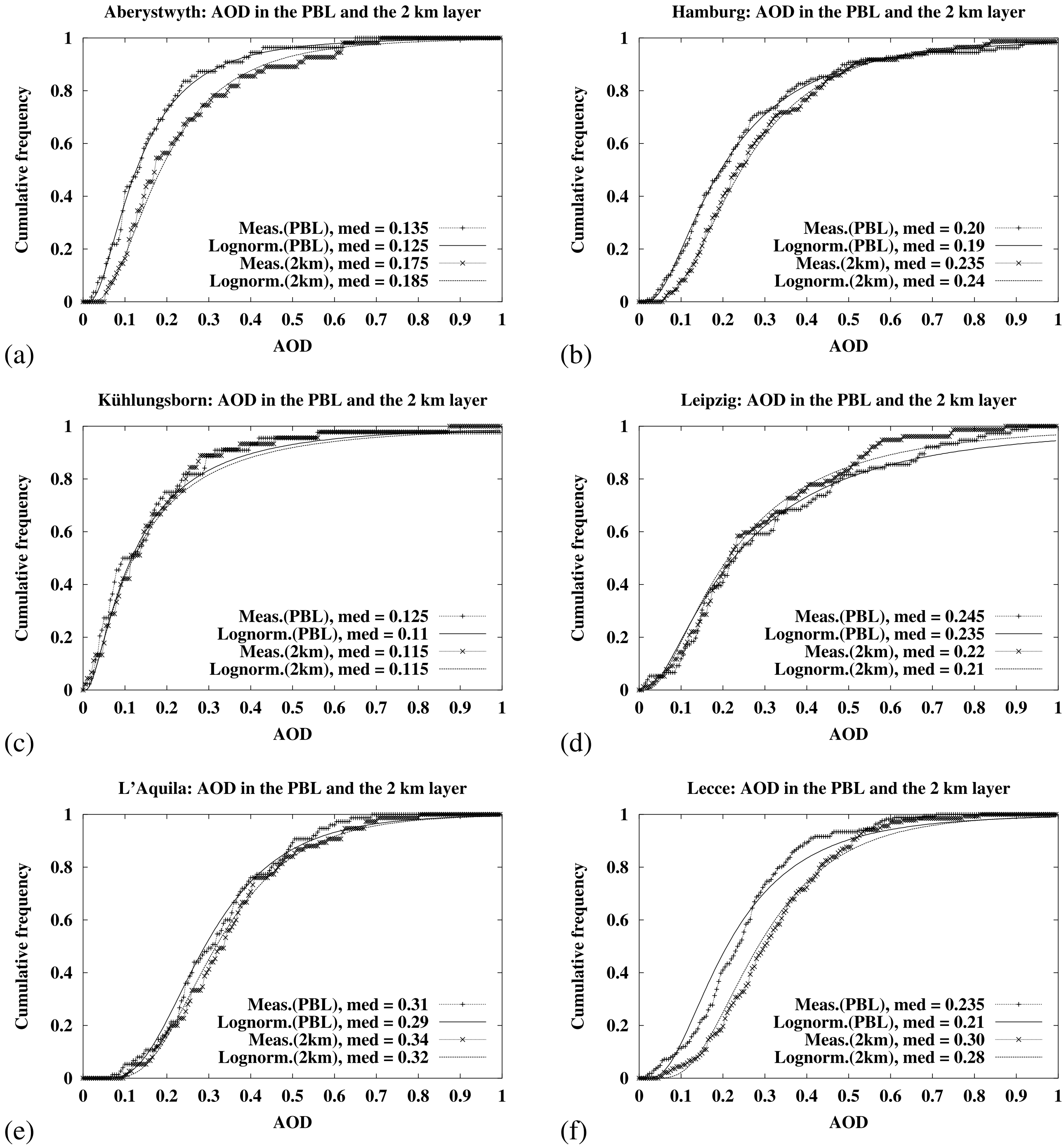

Figure 5. Cumulative frequency distribution of the aerosol optical depth in the PBL and the 2 km layer for 10 EARLINET stations.

5 km is in some cases only represented by a few profiles (Table 1). The corresponding means from Athens in the 2–5 km layer and from Kühlungsborn in the 0–1 km layer are omitted in Figure 6. The mean optical depth values can be calculated by multiplying the mean extinction coefficient with the thickness of the layers.

[30] Figure 6 gives interesting results about the vertical aerosol distribution in northern Europe (represented by Aberystwyth, Hamburg, and Leipzig) compared to southern Europe, especially Italy. Mean extinction coefficients in the 0–1 km and 1–2 km layer are comparable, although there are some differences between the stations in one region of the continent. On average, the Italian stations show larger aerosol extinction coefficients for the 2–5 km layer than the northern stations. The high values in the upper layer represent frequent transport of aerosol at higher altitudes, e.g., from Saharan dust outbreaks or other continental sources and from more efficient convective mixing.

[31] The northern stations show more or less the same vertical distribution of the aerosol extinction coefficient; between 80 and 90% of the total AOD is confined in the lowest 2 km. In Italy about 60–75% of the AOD can be

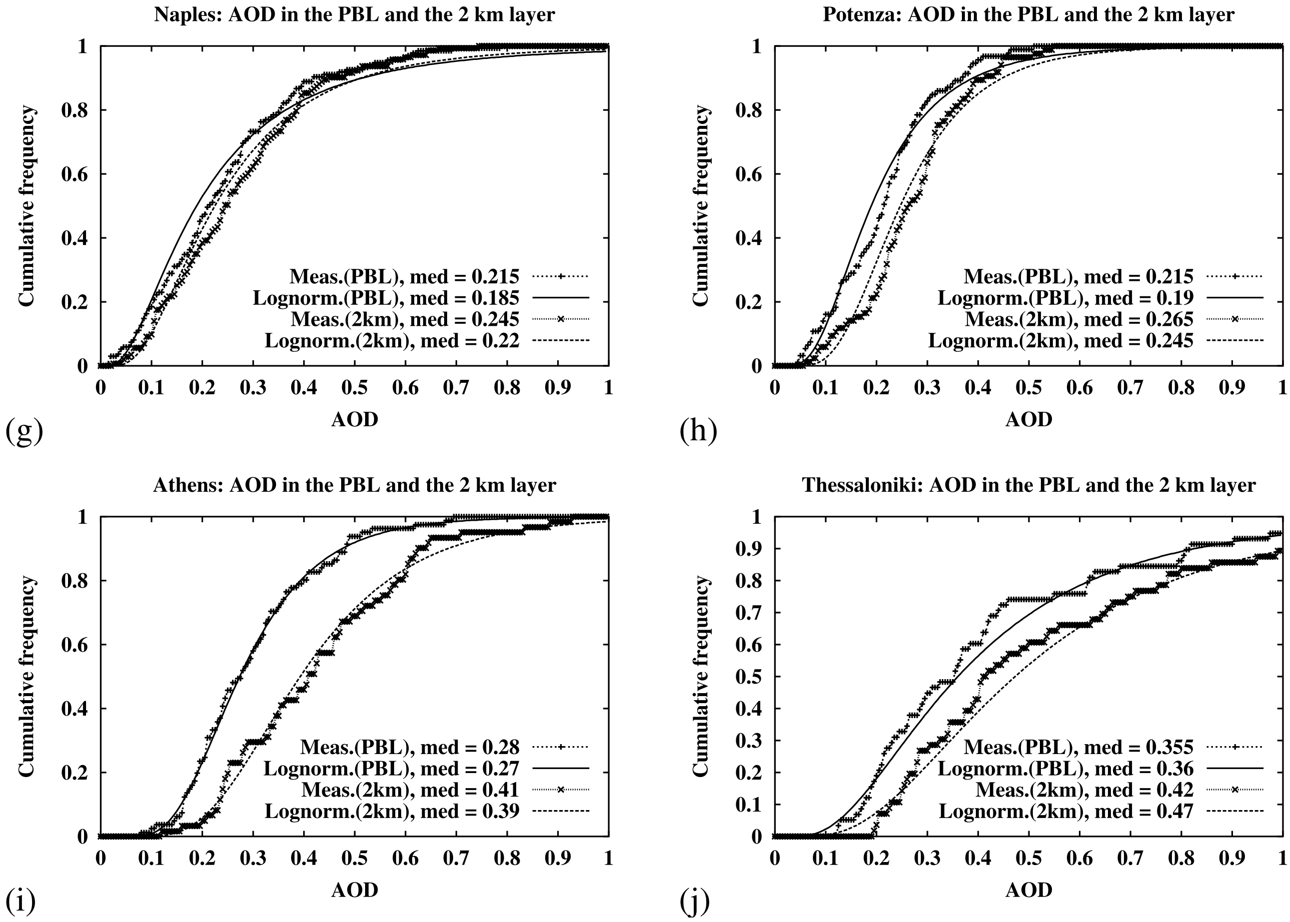

Figure 5. (continued)

found in the lowest 2 km. The two Greek stations show highest values in the lower two layers compared to all other stations. AOD is larger than 0.4 in the lowest 2 km and also the 2–5 km layer shows a large amount of aerosol over Thessaloniki. Here, about 75% of the total AOD can be found below 2 km.

[32] In all layers, a high variability among the profiles can be found. The standard deviation of the individual values is on the order of 50–80% and can reach more than 100% in the 2–5 km layer. The standard deviation of the mean is typically between 5 and 10%. The used data set is large enough so that the differences between the mean aerosol extinction coefficients in the different layers at northern and southern European stations are significant. However, sampling errors caused by different technical setups, measurement strategies, averaging procedures and local weather conditions can also be of some importance. They are not included in the given error margins.

5. Summary

[33] A first statistical analysis of vertical profiles of the aerosol extinction coefficient derived from regular lidar measurements on a continental scale was carried out.

Table 4. Statistical Parameters of the Cumulative Frequency Distribution of the Aerosol Optical Depth in the PBL for 10 EARLINET Stations

	Median of AOD (Measured)		Median of AOD (Fitted)		SD (Log Scale)		1 σ Interval	
Station	PBL	2 km	PBL	2 km	PBL	2 km	PBL	2 km
Aberystwyth	0.135	0.175	0.125	0.185	0.77	0.67	0.06–0.27	0.09–0.36
Hamburg	0.20	0.235	0.19	0.24	0.79	0.62	0.09–0.42	0.13–0.45
Kühlungsborn	0.125	0.115	0.11	0.115	1.00	1.03	0.04–0.31	0.04–0.33
Leipzig	0.235	0.22	0.22	0.21	0.94	0.84	0.09–0.57	0.09–0.49
L'Aquila	0.31	0.34	0.29	0.32	0.49	0.46	0.18–0.47	0.20–0.50
Lecce	0.235	0.30	0.21	0.28	0.67	0.52	0.11–0.41	0.17–0.48
Naples	0.215	0.245	0.185	0.22	0.79	0.65	0.08–0.41	0.12–0.42
Potenza	0.215	0.265	0.19	0.245	0.57	0.47	0.11–0.33	0.15–0.39
Athens	0.27	0.41	0.28	0.39	0.43	0.43	0.18–0.42	0.25–0.60
Thessaloniki	0.355	0.42	0.36	0.47	0.65	0.60	0.19–0.68	0.26–0.86

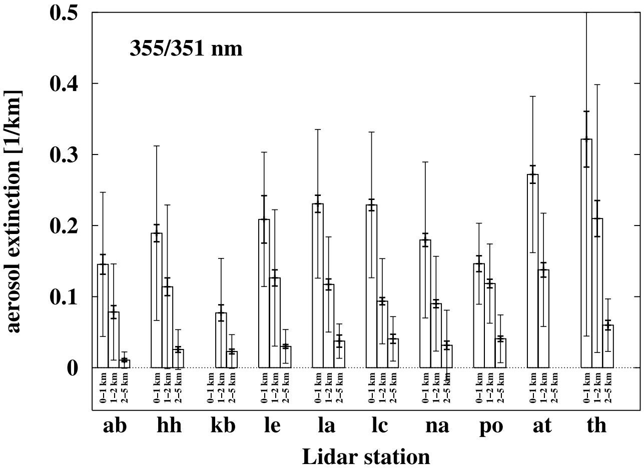

Figure 6. Mean aerosol extinction coefficient in three layers, 0–1 km, 1–2 km, and 2–5 km above ground level. Thin (outer) error bars denote the standard deviation of the individual values, representing the variability between the profiles. Thick (inner) error bars give the standard deviation of the mean.

Lowest values of the aerosol optical depth are found in the northwestern part of Europe (Aberystwyth), highest values in the southeastern part (Athens, Thessaloniki). It could be shown that the increase in aerosol optical depth at the Italian stations is attributed to a higher amount of aerosol in upper layers. Mean AOD values in the lowest 2 km are not significantly larger in Italy than in Germany. However, in Greece the amount of aerosol in the lowest 2 km is significantly larger than at all other stations considered. Higher values at upper altitudes in southern Europe are most likely due to medium- and long-range transport from the Sahara and from other continental sources. Regular EARLINET observations [*Papayannis et al.*, 2002] clearly show a large influence of Saharan dust events on the aerosol distribution in southern Europe.

[34] The aerosol optical depth in the PBL shows an annual cycle with higher values in summer than in winter for most of the stations. Highest values can usually be found in late summer (August/September). The German stations Hamburg, Leipzig and Kühlungsborn show an additional maximum in spring (April). The aerosol optical depth is subject to large fluctuations throughout the whole year. The individual data sets of the investigated EARLINET stations show typical relative standard deviations of 0.4–0.8. High positive skewness of the distributions between typically 0.5 and 1.9 point to a non-Gaussian distribution of the aerosol optical depth values. Statistical tests on the 95% significance level (χ^2 test and Kolmogorov-Smirnov test) show that 9 of the 10 frequency distributions of the AOD in the PBL can be represented by a lognormal distribution. For the 2 km layer, all distribution functions passed the test, if the number of size classes under investigation was appropriately chosen. Consequently, median values represent the statistics much better than mean values do.

[35] The extrapolation of the lowest extinction coefficient to ground to derive aerosol optical depth can be the reason for significant errors in the AOD at some of the stations. The Raman lidar technique allows the determination of the aerosol backscatter coefficient in regions of incomplete overlap. This could be used for an estimate of the aerosol extinction coefficient in low altitudes, but the lidar ratio remains unknown and still has to be estimated in these altitudes.

[36] Regular aerosol lidar measurements give the opportunity to provide a statistics on the PBL height, which can be determined from the range-corrected lidar signal. However, complex aerosol layering or the absence of marked mixing processes can lead to errors in the PBL height determination. In these cases, additional data on e.g., temperature and humidity profiles, which can also be derived by some of the Raman lidar systems, can help to identify the top of the PBL more accurately. Also data from other sensors like radar or sodar or from radio soundings can give valuable information to improve the accuracy of the PBL height statistics.

[37] This statistical analysis yields the first results using a part of the still increasing EARLINET database. The database will be used for further studies about the vertical aerosol distribution over Europe. This includes the statistical analysis of aerosol backscatter coefficients and lidar ratios as well as the identification of main transport patterns by the use of additional back trajectory data.

[38] **Acknowledgment.** The financial support of this work by the European Commission under grant EVR1-CT-1999-40003 is gratefully acknowledged.

References

Andreae, M. O., and P. J. Crutzen (1997), Atmospheric aerosols: Biogeochemical sources and their role in atmospheric chemistry, *Science*, *276*, 1052–1058.

Ansmann, A., U. Wandinger, M. Riebesell, C. Weitkamp, and W. Michaelis (1992), Independent measurement of extinction and backscatter profiles in cirrus clouds by using a combined Raman elastic-backscatter lidar, *Appl. Opt.*, *31*, 7113–7131.

Ansmann, A., U. Wandinger, A. Wiedensohler, and U. Leiterer (2002), Lindenberg Aerosol Characterization Experiment 1998 (LACE 98): Overview, *J. Geophys. Res.*, *107*(D21), 8129, doi:10.1029/2000JD000233.

Balis, D., V. Amiridis, C. Zerefos, E. Gerasopoulos, M. Andreae, P. Zanis, A. Kazantzidis, S. Kazadzis, and A. Papayannis (2003), Raman lidar and sunphotometric measurements of aerosol optical properties over Thessaloniki, Greece during a biomass burning episode, *Atmos. Environ.*, *37*, 4529–4538.

Bates, T., B. Huebert, J. Gras, F. Griffiths, and P. Durkee (1998), International Global Atmosphere Chemistry (IGAC) Project's First Aerosol Characterization Experiment (ACE 1): Overview, *J. Geophys. Res.*, *103*, 16,297–16,318.

Böckmann, C., et al. (2004), Aerosol lidar intercomparison in the framework of the EARLINET project. 2. Aerosol backscatter algorithms, *Appl. Opt.*, *43*, 977–989.

Bösenberg, J., et al. (2001), The German aerosol lidar network: Methodology, data, analysis, *MPI-Rep. 317*, Max-Planck-Inst. für Meteorol., Hamburg, Germany.

Bösenberg, J., et al. (2003), A European aerosol research lidar network to Establish an aerosol climatology, *MPI-Rep. 348*, Max-Planck-Inst. für Meteorol., Hamburg, Germany.

Charlson, R. J., S. E. Schwartz, J. M. Hales, R. D. Cess, J. A. Coakley Jr., J. E. Hansen, and D. J. Hofmann (1992), Climate forcing by anthropogenic aerosols, *Science*, *255*, 423–430.

Coulter, R. L. (1979), A comparison of three methods for measuring mixing-Layer height, *J. Appl. Meteorol.*, *18*, 1495–1499.

De Tomasi, F., A. Blanco, and M. R. Perrone (2003), Raman lidar monitoring of extinction and backscattering of African dust layer and dust characterization, *Appl. Opt.*, *42*, 1699–1709.

Flamant, C., J. Pelon, P. Flamant, and P. Durand (1997), Lidar determination of the entrainment zone thickness at the top of the unstable marine atmospheric boundary layer, *Boundary Layer Meteorol.*, *83*, 247–284.

Intergovernmental Panel on Climate Change (IPCC) (2001), *Climate Change 2001: The Science of Climate Change, Technical Summary of the Working Group I Report*, Cambridge Univ. Press, New York.

Johnson, N., and F. C. Leone (1964), *Statistics and Experimental Design in Engineering and the Physical Sciences*, vol. 1, pp. 213–297, John Wiley, Hoboken, N. J.

Kaimal, J. C., N. L. Abshire, R. B. Chadwick, M. T. Decker, W. H. Hooke, R. A. Kropfli, W. D. Neff, F. Pasqualucci, and P. H. Hildebrand (1982), Estimating the depth of the daytime convective boundary layer, *J. Appl. Meteorol.*, *21*, 1123–1129.

Kalabokas, P., A. Papayannis, A. Chaloulakou, P. Kassomenos, G. Chourdakis, G. Tsaknakis, A. Serafetinides, and N. Spyrellis (2002), On the correlation of gaseous air pollutants with suspended aerosol levels monitored by particle counters and a 2-wavelength lidar system during Saharan dust episodes over the city of Athens, paper presented at IGAC 2002, Int. Assoc. of Meteorol. of Atmos. Sci., Crete, Greece, 18–25 Sept.

Kaufman, Y. J., et al. (1997), Passive remote sensing of tropospheric aerosol and atmospheric correction for the aerosol effect, *J. Geophys. Res.*, *102*, 16,815–16,830.

Lohmann, U., and J. Feichter (1997), Impact of sulphate aerosols on albedo and lifetime of clouds: A sensitivity study with the ECHAM4 GCM, *J. Geophys. Res.*, *102*, 13,685–13,700.

Matthias, V., and J. Bösenberg (2002), Aerosol climatology for the planetary boundary layer derived from regular lidar measurements, *Atmos. Res.*, *63*, 221–245.

Matthias, V., et al. (2004), Aerosol lidar intercomparison in the framework of the EARLINET project. 1. Instruments, *Appl. Opt.*, *43*, 961–976.

Menut, L., C. Flamant, J. Pelon, and P. Flamant (1999), Urban boundary-layer height determination from lidar measurements over the Paris area, *Appl. Opt.*, *38*, 945–954.

Murayama, T., et al. (2001), Ground-based network observations of Asian dust events of April 1998 in East Asia, *J. Geophys. Res.*, *106*, 18,346–18,359.

O'Neill, N. T., A. Ignatov, B. N. Holben, and T. F. Eck (2000), The log-normal distribution as a reference for reporting aerosol optical depth statistics: Empirical tests using multi-year, multi-site AERONET sunphotometer data, *Geophys. Res. Lett.*, *27*, 3333–3336.

Papayannis, A., et al. (2001), Simultaneous observations of free tropospheric Saharan dust layers over Europe monitored by a co-ordinated ground-based lidar network in frame of the EARLINET project, *J. Aerosol Sci.*, *32*(S1), 389–390.

Papayannis, A., et al. (2002), Two years of continuous observations of Saharan dust events over the European continent using a coordinated LIDAR Network in the frame of the EARLINET Project, in *ILRC Lidar Remote Sensing in Atmospheric and Earth Sciences, Reviewed and Revised Papers Presented at the 21st International Laser Radar Conference*, pp. 309–312, Defence R&D Canada—Valcartier, Valcartier.

Pappalardo, G., et al. (2004), Aerosol lidar intercomparison in the framework of the EARLINET project. 3. Raman lidar algorithm for aerosol extinction, backscatter and lidar ratio, *Appl. Opt.*, in press.

Raes, F., T. Bates, F. McGovern, and M. Van Liedekerke (2000), The 2nd Aerosol Characterization Experiment (ACE-2): General overview and main results, *Tellus, Ser. B*, *52*, 111–125.

Russell, P. B., E. E. Uthe, F. L. Ludwig, and N. A. Shaw (1974), A comparison of atmospheric structure as observed with monostatic acoustic sounder and lidar techniques, *J. Geophys. Res.*, *79*, 5555–5566.

Russell, P. B., P. V. Hobbs, and L. Stowe (1999), Aerosol properties and radiative effects in the United States East Coast haze plume: An overview of the Tropospheric Aerosol Radiative Forcing Observational Experiment (TARFOX), *J. Geophys. Res.*, *104*, 2213–2222.

Schwartz, S. E., and A. Slingo (1996), Enhanced shortwave cloud radiative forcing due to anthropogenic aerosols, in *Clouds, Chemistry and Climate, NATO ASI Ser.*, *Ser. I*, vol. 35, edited by P. J. Crutzen and V. Ramanathan, pp. 191–236, Springer-Verlag, New York.

Twomey, S. (1977), Influence of pollution on the short-wave albedo of clouds, *J. Atmos. Sci.*, *34*, 1149–1152.

Wandinger, U., and A. Ansmann (2002), Experimental determination of the lidar overlap profile with Raman lidar, *Appl. Opt.*, *41*, 511–514.

D. Balis, Aristotele University of Thessaloniki, Laboratory of Atmospheric Physics, Box 149, GR-54124 Thessaloniki, Greece. (balis@auth.gr)

J. Bösenberg, Max-Planck-Institut für Meteorologie, Bundesstrasse 55, D-20146 Hamburg, Germany. (boesenberg@dkrz.de)

R. Eixmann, Leibniz-Institut für Atmosphärenphysik, Schlossstrasse 66, D-18225 Kühlungsborn, Germany. (eixmann@iap-kborn.de)

M. Iarlori, Universitá Degli Studi-L'Aquila, Dipartimento di Fisica, Via Vetoio Localitá Coppito, I-67010 L'Aqulia, Italy. (marco.iarlori@aquila.infn.it)

L. Komguem, Physics Department, University of Wales, Aberystwyth, Ceredigion, SY23 3BZ, UK. (llk@aber.ac.uk)

V. Matthias, GKSS Research Center, Institute for Coastal Research, Max-Planck-Strasse 1, 21502 Geesthacht, Germany. (matthias@gkss.de)

I. Mattis, Leibniz-Institut für Troposphärenforschung, Permoserstrasse 15, D-04318 Leipzig, Germany. (ina@tropos.de)

A. Papayannis, National Technical University of Athens, Lasers and Applications Group (LAG-LIDAR Group), Heroon Polytechniou 9, GR-15780 Zografou, Greece. (apdlidar@central.ntua.gr)

G. Pappalardo, Istituto di Metodologie per l'Analisi Ambientale, CNR, Area della Ricerca di Potenza, Contrada S. Loja, I-85050 Tito Scalo, Italy. (pappalardo@imaa.cnr.it)

M. R. Perrone, Dipartimento di Fisica, Universitá di Lecce, via Arnesano, I-73100 Lecce, Italy. (perrone@le.infn.it)

X. Wang, Istituto Nazionale per la Fisica della Materia, Complesso Universitario di Monte S. Angelo ed. G, via Cintia, I-80126 Napoli, Italy. (wang@na.infn.it)